STUDY OF THE MOTION OF POWDER-GAS MIXTURES IN PIPES

Z. M. Kudryavtseva

Inzhenerno-Fizicheskii Zhurnal, Vol. 10, No. 1, pp. 78–85, 1966

UDC 532.529.5

A set of differential hydrodynamic equations is derived for motion of a powder-laden flow in a pipe of variable cross section with allowance for gas compressibility and heat transfer between the components. The characteristics of the motion of mixtures in nozzles and under steady conditions of gas-pressure transport are demonstrated.

The employment in the metallurgical industry of a new process for treating molten metal with powdered reagents introduced in a gas stream has made it necessary to design powder feeding devices characterized by near-sonic mixture outlet velocities. In this connection an attempt has been made to derive a set of simplified hydrodynamic equations based on the principles of motion of each component in a form convenient for solution on a computer.

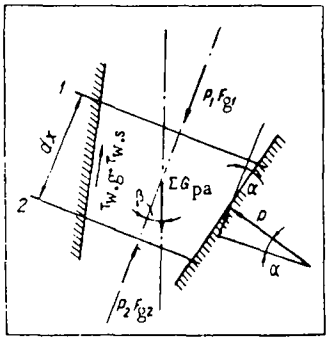

Fig. 1. Diagram of forces acting on an elementary cone.

Allowance has been made for carrier-gas compressibility and also for heat transfer between phases, while the calculations relate to a conical pipe with central convergence angle 2α.

The results of numerous investigations of gas-pressure transport of loose material show that at flow velocities exceeding 15–20 m/sec the solid particles move in a suspended state [1, 2, 3] along nearly rectilinear paths [1, 4], fairly uniformly distributed over the cross section [1, 2, 5]. These conditions ensure the stablest transport without obstruction of the pipe. This permits the following assumptions: a) the flow is one-dimensional and uniformly dispersed over the cross section; b) there is almost no collision between particles. In deriving the equations we also assume that there is no heat exchange with the external medium and that the process is steady and the particles are spherical.

In investigating the hydrodynamics of a two-phase flow allowance is usually made for the reduction of gas flow area in the pipe due to the presence of the second phase:

$$F_g = F - F_s = \varphi F. \tag{1}$$

The equations of continuity of the components and the equation of state of the gas are

$$dG_g = d(F_g \rho_g W_g) = 0; \tag{2}$$

$$dG_s = d(F_s \rho_s W_s) = 0; \tag{3}$$

$$dP = R(\rho_g dT_g + T_g d\rho_g) = 0. \tag{4}$$

The equation of motion of a solid particle is

$$\frac{G_{Pa}}{g} W_s \frac{dW_s}{dX} = \zeta_f \frac{\pi d_s^2}{4} \frac{\rho_g (W_g - W_s)^2}{2g} + G_{Pa} \cos\beta. \tag{5}$$

The particle drag ζ_f varies over the tube length and depends on the Reynolds number referred to the difference of velocity between the components.

The equation of momentum of the mixture is

$$G_g dW_g + \varkappa G_g dW_s = -d(PF_g) + PdF - (\tau_g + \tau_s)\pi D dX + \varkappa g G_g \cos\beta \frac{dX}{W_s}. \tag{6}$$

The first term on the right side of the equation is the pressure acting on opposite sides of an element of the cone (Fig. 1); PdF is the projection on the axis of motion of the pressure on the lateral surface of the jet; $(\tau_g + \tau_s)\pi DdX$ is the friction of the gas and particles against the pipe wall; $\varkappa G_g g \cos\beta\, dX/W_s$ is the gravity force acting on the solid particles in projection on the axis of motion. It is convenient to relate the tangential stresses produced by the solid particles to the concentration of solid particles in the gas [6], having expressed them by analogy with the gas in the form: $\tau_s = \zeta'_{fr.s} \varkappa \rho_g W_g^2/2g$. Values of the wall friction for solid particles $\zeta_{fr.s} = 4\zeta'_{fr.s}$ are given in [6] for several materials and they can also be determined by comparing theoretical calculations with experimental results. In order to determine the coefficient of gas friction against the walls use can be made of ordinary formulas for smooth pipes [2].

The equation for the energy of the mixture referred to 1 kg of gas is

$$c_p dT_g + \frac{dW_g^2}{2} + \varkappa c_s dT_s + \varkappa \frac{dW_s^2}{2} = 0. \tag{7}$$

The equation for heat transfer between the surface of the particles and the gas is

$$-\alpha(T_s-T_g)\pi d_s^2\frac{dX}{W_s}=c_s\rho_s\frac{1}{6}\pi d_s^3 dT_s, \quad (8)$$

where

$$\alpha=\lambda_g 0.2\,\mathrm{Re}_s^{0.83}/d_s;\ \mathrm{Re}_s=(W_g-W_s)d_s/\nu.$$

Thus we have eight initial equations and the same number of unknown functions. By conversion to a form convenient for numerical solution on a computor, we obtained the following set of equations presented in dimensionless form in logical succession with respect to the solution of the problem:

$$\varphi=1-N/D^{*2}W_s^*; \quad (9)$$

$$\mathrm{Re}_s=[(W_g^*-W_s^*)P^*\Gamma]\left[\left(\frac{1+c^*/T_0^*}{1+c^*/T_g^*}\right)\sqrt{\frac{T_g^*}{T_0^*}}\,T_g^*\right]^{-1}; \quad (10)$$

$$\zeta_f=24/\mathrm{Re}_s \text{ for } \mathrm{Re}_s<1; \quad (11)$$

$$\zeta_f=24/\mathrm{Re}_s+4.3/\sqrt[3]{\mathrm{Re}_s} \text{ for } 1<\mathrm{Re}_s<3000; \quad (11a)$$

$$\zeta_f=0.42 \text{ for } \mathrm{Re}_s>3000; \quad (11b)$$

$$\frac{dW_\tau^*}{dX_s^*}=\frac{3}{4}\zeta_f B\frac{P^*}{T_g^*}\frac{(W_g^*-W_s^*)^2}{W_s^*}-\frac{\cos\beta}{W_s^*\mathrm{Fr}}; \quad (12)$$

$$\frac{dT_s^*}{dX^*}=\frac{-1.2E\,\mathrm{Re}_s^{0.83}(T_g^*-T_s^*)}{W_s^*}; \quad (13)$$

$$\mathrm{Re}_g=W_g^*D^*\sqrt{\varphi}\,P^*\Gamma'\Big/\left(\frac{1+C^*/T_0^*}{1+C^*/T_g^*}\right)\sqrt{\frac{T_g^*}{T_0^*}}\,T_g^*; \quad (14)$$

$$\zeta_{fr.g}=\left[\frac{0.55}{\lg\frac{\mathrm{Re}_g}{8}}\right]^2; \quad (15)$$

$$\frac{dW_g^*}{dX^*}=\left[-\varkappa\frac{c_s}{c_p}\frac{dT_s^*}{dX^*}+(\zeta_{fr.g}+\varkappa\zeta_{fr.s})\frac{k}{k+1}\frac{W_g^{*2}}{\varphi D^*}+\frac{4T_g^*}{\varphi D^*}\operatorname{tg}\alpha\right]\times\left[\frac{2}{k+1}W_g^*\left(\frac{k+1}{2}\frac{T_g^*}{W_s^{*2}}-1\right)\right]^{-1}+$$

$$+\left[\varkappa\frac{2k}{k+1}\left[W_g^*-W_s^*\frac{k-1}{k}\right]\frac{dW_s^*}{dX}+\frac{2k}{k+1}\varkappa\frac{W_g^*}{W_s^*}\frac{\cos\beta}{\mathrm{Fr}}\right]\times\left[\frac{2}{k+1}W_g^*\left(\frac{k+1}{2}\frac{T_g^*}{W_g^{*2}}-1\right)\right]^{-1}; \quad (16)$$

$$-\frac{dP^*}{dX^*}=\frac{2k}{k+1}\frac{W_g^*P^*}{T_g^*}\left\{\frac{dW_g^*}{dX^*}+\left[\varkappa+\frac{Tg}{W_s^*W_g^*}\frac{(1-\varphi)}{\varphi}\frac{k+1}{2k}\right]\frac{dW_s^*}{dX^*}+(\zeta_{fr.g}+\varkappa\zeta_{fr.s})\frac{W_g^*}{2\varphi D^*}-\frac{\cos\beta}{\mathrm{Fr}}\frac{\varkappa}{W_s^*}\right\}; \quad (17)$$

$$\frac{dT_g^*}{dX^*}=-\frac{T_g^*dW_g^*}{W_g^*dX^*}+\frac{T_g^*dP^*}{P^*dX^*}+\frac{(1-\varphi)T_g^*dW_s^*}{\varphi W_s^*dX^*}-\frac{4T_g^*}{\varphi D^*}\operatorname{tg}\alpha; \quad (18)$$

$$\frac{dD^*}{dX^*}=-2\operatorname{tg}\alpha. \quad (19)$$

All the quantities in the equations represent ratios of the variable flow parameters to the corresponding scales for which we chose the initial gas stagnation temperature T_{g01}, the critical gas velocity corresponding to T_{g01}, the initial gas pressure P_1, the pipe diameter at the inlet D_1, and the thermal conductivity of the gas under normal conditions λ_0:

$$T_s^*=T_s/T_{g01};\ T_g^*=T_g/T_{g01};\ W_s^*=W_s/W_{cr1};$$

$$W_g^*=W_g/W_{cr1};\quad P^*=P/P_1;$$

$$X^*=X/D_1;\ D^*=D/D_1;\ T_0^*=T_0/T_{g01}=$$

$$=273/T_{g01};\ C^*=C/T_{g01};$$

Γ, Γ', N, E, Fr, and B are constants for the given problem and are expressed by the following relationships:

$$\Gamma=\frac{2k}{k+1}\frac{d_s P_1}{\mu_0 W_{cr1}};\quad \Gamma'=\frac{\Gamma D_1}{d_s};\quad N=\frac{G_s}{\rho_s W_s F_1};$$

$$E=\frac{D_1\lambda_0}{d_s^2\rho_s c_s W_{cr1}};\ \mathrm{Fr}=\frac{W_{cr1}}{gD_1};\quad B=\frac{\rho_{g1}}{\rho_g}\frac{D}{d_s}.$$

The system of equations was programmed for solution on the M-2 computer.

By comparing the results of calculations with experimental data (table) one can check how accurately the system of equations obtained describes the true process.

Experiments nos. 7–10 were carried out on a special experimental device which made it possible to check the method under conditions of high pressure and sonic gas jet velocity at atmospheric pressure in the outlet cross section. During the experiments measurements were made of the flow rates of the components, their temperatures, gas pressure at different cross sections over the length of experimental part of the channel, and the reaction of the jet. The particle velocity at the outlet was determined from Euler's equation:

$$P_{\text{react}}=\frac{G_g}{g}W_{g2}-\frac{G_s}{g}W_{s2} \quad (20)$$

The first calculations for experiments nos. 1 and 4 were carried out on the assumption that the wall friction $\zeta_{fr.s}=0$. This made it possible to determine the actual value of $\zeta_{fr.s}$ by comparing the

Characteristics of Experimental Data Used in Computer Calculations

No. of expt.	Gas	Material	Density, kg/m³	Particle diam., mm	Pipe length, mm	Initial pressure, N/m²	Mass flow rate of gas, kg/min	Concentration, kg/kg	Remarks
1	air	wheat	1220	3.0	89.0	$0.99 \cdot 10^5$	8.05	14.6	experiments no. 20
2							9.45	6.27	of Gastershtadt
3							9.25	3.7	[1] no. 25
4	"	ash from	1500	average	41.12	$1.142 \cdot 10^5$	1.68	2.67	Uspenskii's
5		Chelyabinsk coal	"	0.142	"	$1.36 \cdot 10^5$	3.04	1.642	experiments
6		coal dust	1350	" 0.105	"	$1.118 \cdot 10^5$	1.65	2.755	
7		calcium	4000	fine	4.0	$4.51 \cdot 10^5$	0.352	7.0	TsNIIChM's
8	nitrogen	ferrite		fraction		$3.13 \cdot 10^5$	0.350	2.7	experiments
9						$4.11 \cdot 10^5$	0.250	12.0	(at sonic gas
10				0.14–0.2		$2.745 \cdot 10^5$	0.352	8.5	outlet velocities)

results of calculation with experimental data, on the assumption that the portion of the losses not taken into account equals the difference between the predicted and the experimental pressure drops.

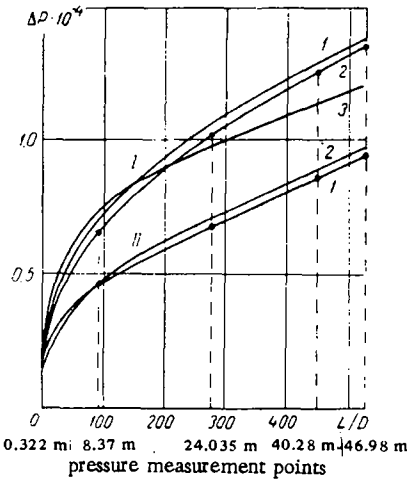

Fig. 2. Variation in gas pressure ΔP, N/m^2, over tube length in experiments nos. 1 and 2 ([1], experiments no. 20 and 25): 1) experiment; 2) calculation with $\zeta_{fr.s} = 0.0061$; 3) calculation with $\zeta_{fr.s} = 0$; I) at $\varkappa = 1.46$; II) $\varkappa = 6.27$.

As a result of such a comparison we obtained: for Gastershtadt's experiments $\zeta_{fr.s} = 0.00161$; for Uspenskii's experiments $\zeta_{fr.s} = 0.0025$ (which is in complete agreement with the data given in [6]). When a mixture moves at high velocity the role of losses due to friction in the over-all power balance is small, therefore in this case $\zeta_{fr.s}$ was taken as zero.

The results of calculations with the above-mentioned coefficients $\zeta_{fr.s}$ are shown in Figs. 2, 3, and 4. It follows from plot 4 that the variation of the parameters of a gas moving with suspended solid particles is identical with their variation for a pure gas [7]. The gas reaches sonic velocity only at the end of the pipe whose length is uniquely defined by the boundary conditions of the problem. Therefore the pipe length is an object for comparison of calculation and experiment, together with such characteristics as the pressure gradients over the flow length and the particle velocity. Despite the quite different initial conditions of the problems, the results of solving them in all the cases considered prove to be very similar to the experimental results and correctly represent the actual process: the difference between calculation and experiment in respect of these characteristics amounts to 2–7%.

A comparison of the curves in Figs. 3 and 4 shows that the aerodynamics of the mixture is essentially different in all three cases.

By calculating numerous versions of the problem on a computer a number of special features of powder-laden flow in nozzles at sonic gas exit velocities have been established, namely;

1. Coefficient of resistance of powder-laden flow in nozzles increases: a) with decrease in ρ_s and d_s due to increase in velocity gradient $(dW_s)/(dX)$, b) with decrease in the particle velocity at the nozzle inlet, c) with increase in initial particle temperature, which causes an increase in the temperature and velocity of the gas during motion.

2. The particle velocity at the nozzle outlet is considerably lower than the gas velocity, amounting to 15/100–45/100 of the sonic velocity in the cases investigated. The particle outlet velocity can be increased by raising initial gas pressure and increasing nozzle length.

3. Comparison of the energy balances for the individual stages of a moving mixture showed that in this case the basic losses of gas energy are associated with an increase in the kinetic energy of both phases. The specific value of losses due to friction is not greater than 5–7%. Therefore at $\varkappa = 4$–5 the pipe diameter has no significant effect on the aerodynamics of the nozzle.

The nomogram shown in Fig. 5 makes it possible to determine nozzle inlet gas pressure and nozzle outlet particle velocity from the given concentration and nozzle length. The nomogram can be used for designing nozzles from 6 to 35 –40 mm in diameter.

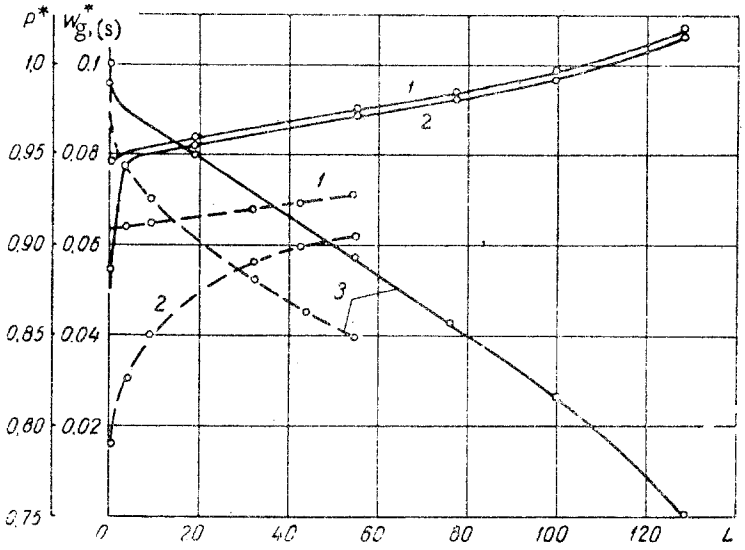

Fig. 3. Variation in the velocity of the components $W_g^* = W_g/W_{cr}$ (1), $W_s^* = W_s/W_{cr}$ (2) and in pressure $P^* = P/P_1$ (3) over pipe length L, m, from the results of experiments No. 1 (broken lines) and No. 5 (continuous lines).

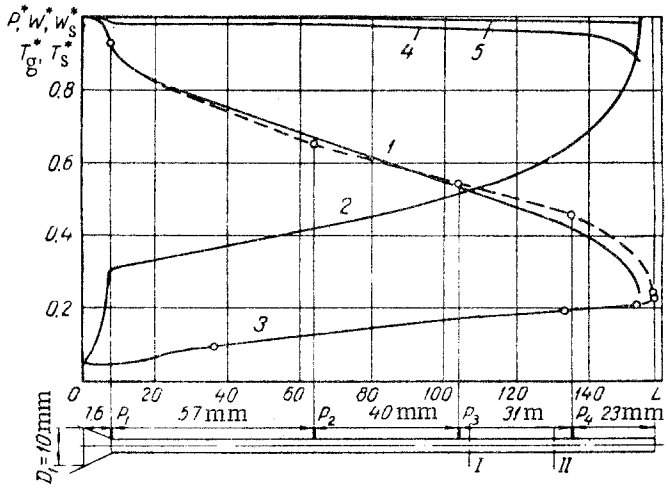

Fig. 4. Variations in dimensionless parameters of the mixture P* (1), W_g^* (2), W_s^* (3), T_g^* (4), T_s^* (5) over the experimental pipe length L, mm, at sonic gas outlet velocity according to the design data of experiment No. 7 (W_{cr1} = 312 m/sec, $P_1 = 4.51 \times 10^5$ N/m^2, T_{g01} = 283° K, $\varkappa$ = 7). Continuous line–calculation; broken line–experiment.

The special features of the aerodynmaics of mixtures at low velocities follow from the results of calculations for velocities of about 20 m/sec, shown in Fig. 3, namely:

1. The length of the particle acceleration path is the greater, the larger the particles. Thus, at d_s = = 3 mm, 0.142 mm, 5μ it is 450, 30, and 0.25 calibers, respectively.

2. Immediately beyond the acceleration sector conditions are characterized by equality of the velocity gradients for the two components

$$\frac{dW_g}{dX} = \frac{dW_s}{dX}, \qquad (21)$$

this equality is very stable for these powders.

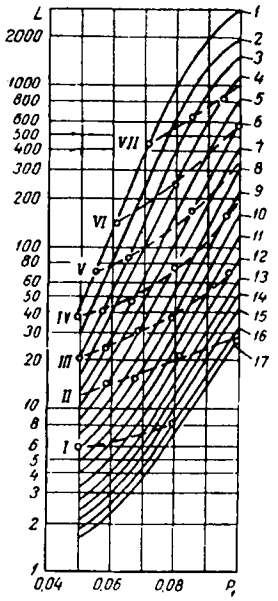

Fig. 5. Nomogram designing nozzles intended for feeding powdered lime in a jet of natural gas (P_1 in MN/m^2; L in mm, $\varkappa$ in kg/kg): 1) W^*_s = 0.15; II) 0.20; III) 0.25; VI) 0.30; V) 0.35; VI) 0.40; VII) 0.45; 1) $\varkappa$ = 4; 2) 5; 3) 6; 4) 7; 5) 8; 6) 9; 7) 10; 8) 11; 9) 12; 10) 13; 11) 14; 12) 15; 13) 16; 14) 17; 15) 18; 16) 19; 17) 20.

3. Unlike the motion of mixtures in nozzles, the greatest part of the gas energy under equal-gradient conditions is expended in overcoming the friction of gas and particles against the walls, and, under conditions of particle acceleration, in increasing their velocity. However, as the distance from the inlet increases, the expenditure of energy on acceleration decreases, and the part played by losses due to friction increases.

Introducing condition (21) into the set of equations (9)–(19) and neglecting heat transfer between phases, we obtain an equation for determining the difference in velocity under equal-gradient conditions of gas-pressure transport $\Delta W = W_g - W_s$, which in dimensional form is as follows:

$$\frac{\varkappa(k-1)}{W_g}\Delta W^3 - \left(\frac{W_{sn}^2}{W_g^2} - 1 - \varkappa\right)\Delta W^2 - \frac{2}{3}kW_g(\zeta_{fr.g} + \varkappa\zeta_{fr.s})\Delta W\,St + \frac{2}{3}kW_g^2(\zeta_{fr.g} + \varkappa\zeta_{fr.s})St = 0. \qquad (22)$$

Here

$$St = \frac{1}{\zeta_f}\frac{\rho_s d_s}{\rho_g D}. \qquad (23)$$

For powders the first term of the equation can be neglected; we then have

$$a\Delta W^2 + b\Delta W - bW_g = 0, \qquad (24)$$

where

$$a = \left(\frac{W_{sn}^2}{W_g^2} - 1 - \varkappa\right); \quad b = \frac{2}{3}k(\zeta_{fr.g} + \varkappa\zeta_{fr.s})W_g\,St.$$

Under the same conditions and at $Re_s < 1$, with allowance for Eq. (11),

$$\Delta W = \frac{\rho_s d_s^2 k(\zeta_{fr.g} + \varkappa\zeta_{fr.s})W_g^2/36\mu D}{a + \rho_s d_s^2 k(\zeta_{fr.g} + \varkappa\zeta_{fr.s})W_g/36\mu D}.$$

At $Re_s > 1$ Eq. 24 should be solved with ζ_f of (11a) by the method of successive approximations.

NOTATION

W—velocity; T—temperature; P—pressure; T_{g0}—gas stagnation temperature; D—pipe diameter; d_s—particle diameter; ρ_s—density; G—mass flow rate (in the international system of units); $\varkappa$—mass concentration; G_{pa}—particle mass; φ—portion occupied by gas; ζ_{fr}—wall friction; ζ_f—particle drag; c_s, c_p—specific heat of solid particles and of gas; $k = c_p/c_v$; R = gas constant; μ, ν—dynamic and kinematic viscosity coefficients; g—acceleration due to gravity; τ—tangential stress; C—constant in Sutherland's equation; α—heat transfer coefficient; λ, λ_0—heat conductivity of gas and heat conductivity of gas under normal conditions; β—angle between vertical axis and direction of motion; W_{cr}, W_{sn}—critical and sonic velocity; subscripts s refer to solid phase, g—to gas; 1 and 2 to initial and final cross sections of pipe; asterisks denote dimensionless parameters.

REFERENCES

1. I. Gastershtadt, Pneumatic Transport [in Russian], Izd. Sev.-zap. obl. Prombyuro VSNKh, 1927.

2. V. A. Uspenskii, Pneumatic Transport [in Russian], Metallurgizdat, 1959.

3. E. A. Zhikharev, IFZh, no. 2, 1959.

4. L. D. Batsalko, Study of Seed Transportation Process by Pneumatic Methods [in Russian], Dis. VIM i VIESKh, Moscow, 1960.

5. M. E. Login and V. P. Lebedev. Trudy TEMIIT, 29, 1960.

6. E. Muschelknautz, VDI-Forschungsheft, 25, 476, "B", 1959.

7. M. E. Deich, Engineering Gas Dynamics [in Russian], Gosenergoizdat, Moscow-Leningrad.

9 March 1965

Bardin Ferrous Metallurgy Institute, Moscow